

# A Comparative Study on the Effects of Paper Sludge and Kaolin on Properties of Polypropylene/Ethylene Propylene Diene Terpolymer Composites

Salmah, Hanafi Ismail, and Azhar Abu Bakar

School of Materials and Mineral Resources Engineering,  
Universiti Sains Malaysia, 14300 Nibong Tebal, Penang, Malaysia.

Received 13 June 2004; accepted 22 June 2005

## ABSTRACT

The effects of paper sludge (PS) and kaolin on properties of PP/EPDM composites were examined. The mechanical properties, morphology, water absorption, and thermal properties were investigated. At a similar filler loading, PP/EPDM/kaolin composites show higher mechanical properties (such as tensile strength and elongation at break, except Young's modulus), lower water absorption, and better thermal stability compared to PP/EPDM/PS composites. However PP/EPDM/PS composites exhibit better Young's modulus and percentage of crystallinity than PP/EPDM/kaolin composites. SEM of tensile fracture surfaces of composites show that the PP/EPDM/kaolin composites have better filler dispersion and filler-matrix interaction than PP/EPDM/PS composites.

### Key Words:

paper sludge;  
kaolin;  
polypropylene;  
ethylene propylene diene terpolymer;  
composites.

## INTRODUCTION

A variety of inorganic and organic reinforcing fillers may be incorporated into polypropylene (PP) in order to improve specific properties or reduce cost. Polypropylene (PP) is usually filled with talc, calcium carbonate, and silica to lower the price

and improve properties or provide reinforcement [1-4].

The introduction of particulate mineral fillers into a thermoplastic polymer can improve some mechanical properties such as Young's modulus or the heat deflection tempera-

(\*)To whom correspondence should be addressed.  
E-mail: hanafi@eng.usm.my

ture, but it affects some others properties, like impact strength, adversely. However, these negative effects can be minimized by the use of very fine particles. Because of their small size, these particles tend to agglomerate and impart a good particle dispersion to the matrix, a surface treatment is needed which decrease the strength of the interaction among them.

Many researchers have used natural fibers, such as rubberwood [5-7], palm oil fruit bunch [8-9], jute [10], bamboo [11-12], and conifer [13] as alternative for reinforcing thermoplastics and elastomers, due to their low density, low cost, non-abrasiveness, recyclability, biodegradability, and renewable nature.

Paper sludge (PS), a waste residue from the pulp and paper processing has brought great pressure on the environment because of large quantity produced in paper mills [14-16]. Generally, most of this paper sludge is landfilled and some is incinerated or utilized for farming. Considering the short cellulose fibres and inorganic fillers such as kaolin and calcium carbonate contained in this kind of sludge, there will be wide commercial applications and development prospects for paper sludge as a new kind of filler in polymer processing [17].

This article reports the results of an investigation on the effect of paper sludge loading on the mechanical properties, swelling behaviour, morphology, and thermal properties of PP/EPDM/PS composites. Similar composites but using kaolin as a filler were also prepared for comparison.

## EXPERIMENTAL

### Materials

Polypropylene homopolymer used in this study was of injection molding grade, from Titan PP polymers (M) Sdn Bhd, Johor, Malaysia (code 6331) with MFI value of 14.0 g/10 min at 230°C. Ethylene propylene diene

monomer (EPDM), grade Mitsui EPT 3072 E was obtained from Luxchem Trading Sdn Bhd., Selangor, Malaysia. Paper sludge (PS) which is the waste product of paper mills process was obtained from Nibong Tebal Paper Mill Sdn Bhd, Penang, Malaysia. Paper sludge was dried in a vacuum oven at 80°C for 24 h to make it free from moisture and then grinded to powder. An Endecotts sieve was used to obtain an average filler sizes of 63  $\mu\text{m}$  (density, 2.2  $\text{g}/\text{cm}^3$ ). Kaolin was obtained from Ipoh Ceramic Sdn Bhd., Ipoh, Malaysia, with average size of 9.7  $\mu\text{m}$  (density, 2.2  $\text{g}/\text{cm}^3$ ). The formulation of PP/EPDM/PS and PP/EPDM/kaolin composites used in this study are shown in Table 1. The results of semi-quantitative analysis of paper sludge and kaolin used in this study are shown in Tables 2 and 3.

### Mixing Procedure

Composites were prepared in a Haake Reomix PolyDrive. Mixing was done at 180°C and 50 rpm. The EPDM was first charged to start the melt mixing. After 3 min filler was added followed by PP at the fifth min. Mixing was continued for another 5 min. At the end of 10 min, the composites were taken out and sheeted through a laboratory mill at 2.0 mm nip setting. Samples of composites were compression moulded in an electrically heated hydraulic press. Hot-press procedures involved preheating at 180°C for 6 min followed by compressing for 4 min at the same temperature and subsequent cooling under pressure for 4 min.

### Measurement of Tensile Properties

Tensile tests were carried out according to ASTM D 412 on the Instron 3366. 1 mm thick dumb bell specimens were cut from the moulded sheets with the Wallace die cutter. A cross head speed of 50 mm/min was used and the test was performed at  $25 \pm 3^\circ\text{C}$ .

### Water Absorption Test

The composite samples were immersed in distilled

**Table 1.** Formulation of PP/ EPDM composites with different filler.

Materials	Blends
Polypropylene (PP) (wt%)	50
Ethylene propylene diene terpolymer (EPDM) (wt%)	50
Paper sludge (PS) (wt%)	0, 15, 30, 45, 60
Kaolin (wt%)	0, 15, 30, 45, 60

water at room temperature. The water absorption were determined by weighing the samples at regular intervals. The Mettler balance type AJ150 was used, with a precision of  $\pm 1$  mg. The percentage of water absorption,  $M_t$  was calculated by

$$M_t = \frac{W_N - W_d}{W_d} \times 100 \quad (1)$$

Where  $W_d$  and  $W_N$  are original dry weight and weight after exposure, respectively.

### Morphology Study

Studies on the morphology of the tensile fracture surface of the composites were carried out using a scanning electron microscope (SEM), model Leica Cambridge S-360. The fracture ends of specimens were mounted on aluminium stubs and sputter coated with a thin layer of gold to avoid electrostatic charging during examination.

### Thermogravimetry Analysis

Thermogravimetry analysis of the composites were carried out with the Perkin Elmer Pyris 6 TGA analyzer. The sample weight of about 15-25 mg were scanned from 50 to 600°C using a nitrogen air flow of 50 ml/min and a heating rate of 20°C/min. The sample size was kept nearly the same for all tests.

### Differential Scanning Calorimetry

Thermal analysis measurements of selected systems were performed using a Perkin Elmer DSC-7 analyzer. Samples of about 10-25 mg were heated from 20-220°C using a nitrogen air flow of 50 mL/min and the heating rate of 20°C/min. The melting and crystallization behaviour of selected composites were also performed using a Perkin Elmer DSC-7. The crystallinity ( $X_{com}$ ) of composites were determined using the following relationship:

$$(\% \text{ crystallinity}) X_{com} = \Delta H_f / \Delta H_f^0 \times 100 \quad (2)$$

Where  $\Delta H_f$  and  $\Delta H_f^0$  are enthalpy of fusion of the system and enthalpy of fusion of perfectly (100%) crystalline PP, respectively. For  $\Delta H_f^0$  (PP) a value of 209 J/g was used for 100% crystalline PP homopolymer [18]. However,  $X_{com}$ , which is calculated using

this equation, gives only the overall crystallinity of the composites based on their total weights including non-crystalline fractions, and it is not the true crystallinity of the PP phase. The value of crystallinity for PP phase ( $X_{pp}$ ) of the PP fraction was normalized using eqn (3) as follow [19]:

$$X_{pp} = (X_{com})/Wf_{pp} \quad (3)$$

Where  $Wf_{pp}$  is the weight fraction of PP in the composites.

## RESULTS AND DISCUSSION

The torque-time curves of PP/EPDM/PS and PP/EPDM/kaolin composites with 0, 30, and 60 (wt %) filler loading are shown in Figure 1. In general, all torque-time curves for each composite have a similar pattern, except PP/EPDM curve. At the beginning, EPDM was charged into Haake and rotors were started. A sharp increase in torque was obtained because of the resistance exerted by the EPDM against the rotors. The peak started to decrease as the fusion of EPDM took place. A sharp decrease in the mixing torque was observed immediately after the addition of filler, paper sludge or kaolin at the third minute due to lubricant action of filler. At the fifth minute, at which cold PP was charged into the mixer, a sharp peak was registered. This abrupt rise in torque represents the loading and fusion peak of PP. As fusion of PP is completed,

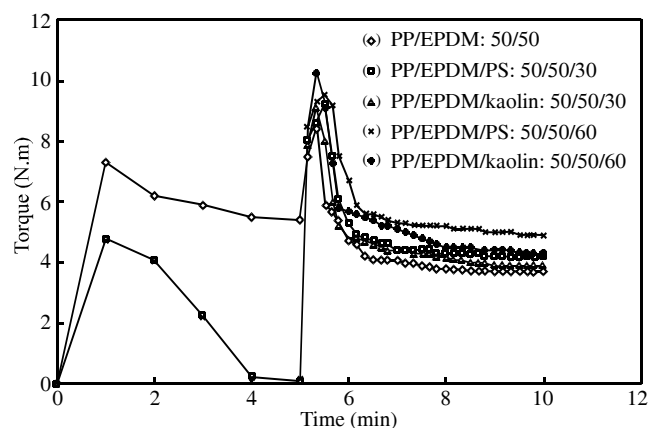


**Figure 1.** Torque vs. time of PP/EPDM, PP/EPDM/PS, and PP/EPDM/kaolin composites with 0, 30, and 60 wt (%) filler loading.

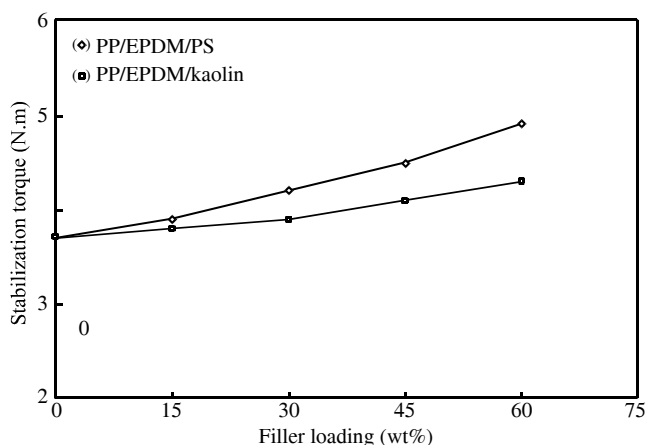


**Figure 2.** Stabilization torque vs. filler loading of PP/EPDM/PS and PP/EPDM/kaolin composites with different filler loading.

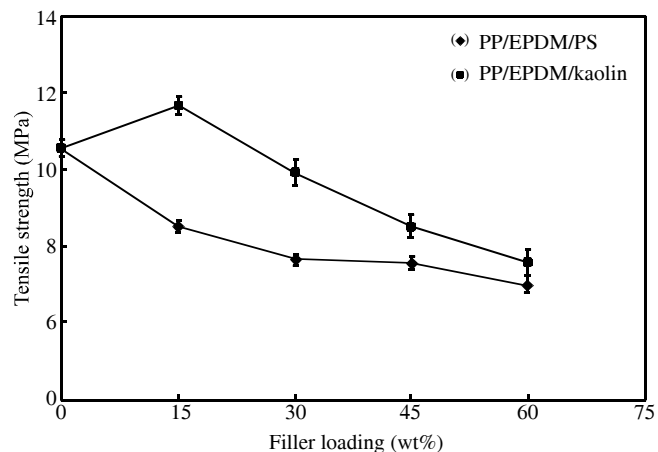
torque started to decrease gradually, due to a decrease in viscosity, until it has adjusted to more stable value.

Figure 2 shows the relationship between stabilization torque and filler loading of PP/EPDM/PS and PP/EPDM/kaolin composites at different filler loading. It can be seen that the stabilization torque increases with increasing filler loading. This indicates that the increasing loading of filler has increased the melt viscosity of the composites. At a similar filler loading, PP/EPDM/PS composites have a higher stabilization torque than PP/EPDM/kaolin composites. This indicates that the addition of paper sludge in PP/EPDM matrix has increased the viscosity the composite and the addition of kaolin has had favourable effect on processing compared to paper sludge

Figure 3 shows the effect of filler loading on tensile strength of PP/EPDM/PS and PP/EPDM/kaolin composites. It can be seen that the tensile strength for both fillers decreases with increasing filler loading.

Figure 4 shows the SEM of the paper sludge at the magnification of 151X. It is clear that paper sludge consists of irregular shape filler particles. In our previous work [20], we have reported that paper sludge consists of various shape and form such as fibres, particulate, etc. For irregular shape fillers the tensile strengths of composites decrease due to the inability of the filler to support stresses transferred from matrix.

Figure 5 shows the SEM of the kaolin at magnification of 1000X. For kaolin, the agglomeration of filler particles can form a domain that acts like body which weakens the filler-matrix interaction particularly when



**Figure 3.** Effect of filler loading on tensile strength of PP/EPDM/PS and PP/EPDM/kaolin composites.



**Figure 4.** Scanning electron micrograph of paper sludge at magnification 151X.

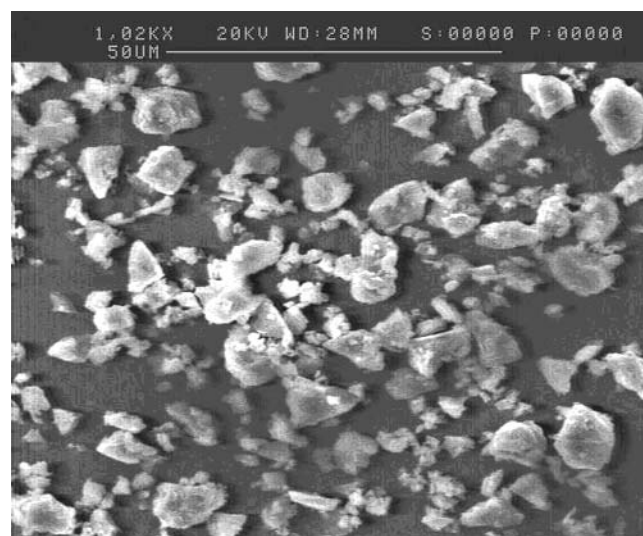


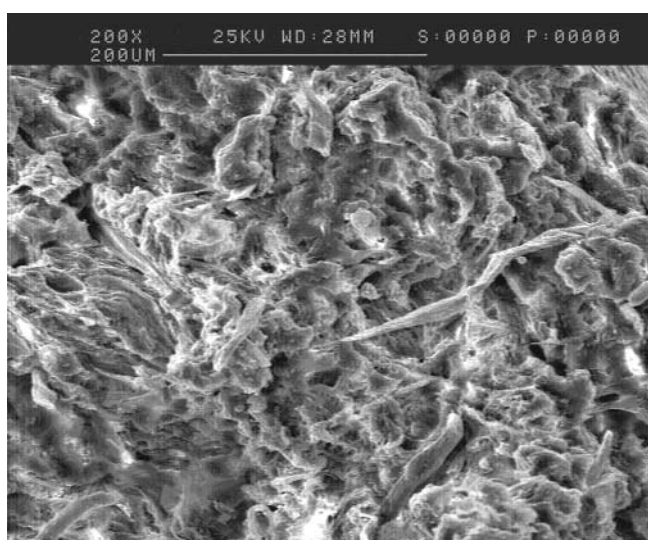
**Figure 5.** Scanning electron micrograph of kaolin at magnification 1000X.

more than 15 (wt%) kaolin was used. At a similar filler loading PP/EPDM/kaolin composites exhibit higher tensile strength than PP/EPDM/PS composites, which can be attributed to the characteristics of the filler. Kaolin has average smaller particle size ( $9.7 \mu\text{m}$ ) than paper sludge ( $63 \mu\text{m}$ ). The smaller size of the filler provides a bigger surface area for better interfacial interaction between filler and matrix [21] which is indicated in the SEMs in Figures 6 and 7.

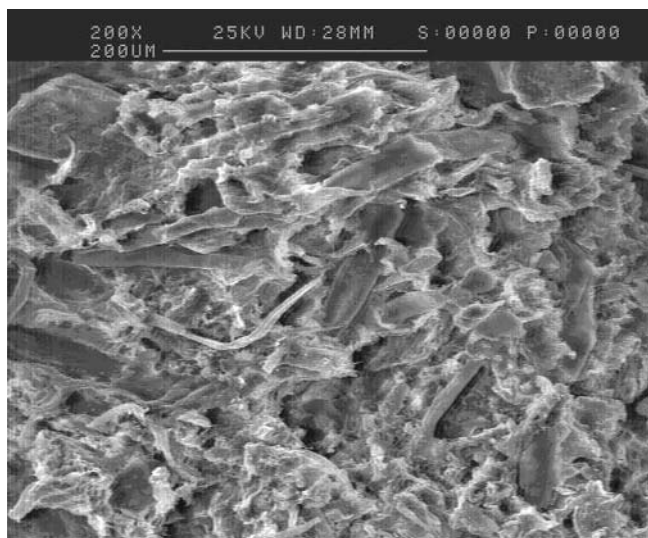
The SEM in Figure 6 (a and b) shows the tensile fracture surface of PP/EPDM/PS composites with 30 and 60 wt% of paper sludge. It can be seen that the frac-

ture surface of composites shows hole and unwetted paper sludge fibre and particulate on the surface particularly at higher filler loading (60 wt%). This indicates poor adhesion occurred between the PP/EPDM matrix and paper sludge.

Figure 7 (a and b) shows fracture surface of PP/EPDM/kaolin composites at 30 and 60 wt% of kaolin. They show better dispersion and wetting and less pull out of filler from matrix compared to PP/EPDM/PS composites (Figures 6a and 6b). Consequently, PP/EPDM/ kaolin composites exhibit better tensile strength (Figures 3) and elongation-at-break

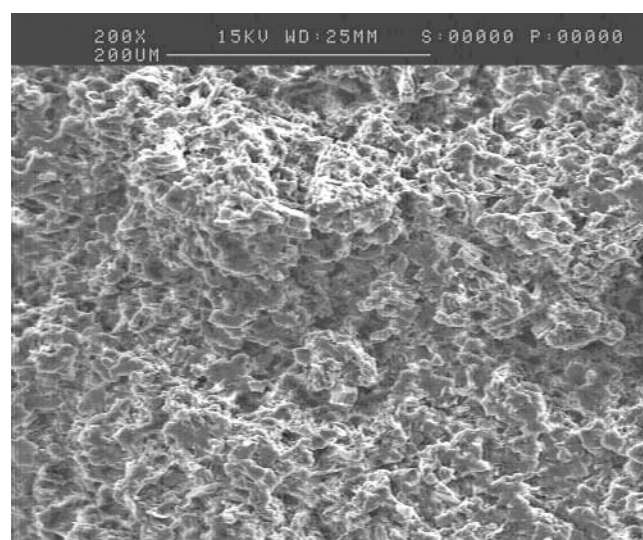


(a)

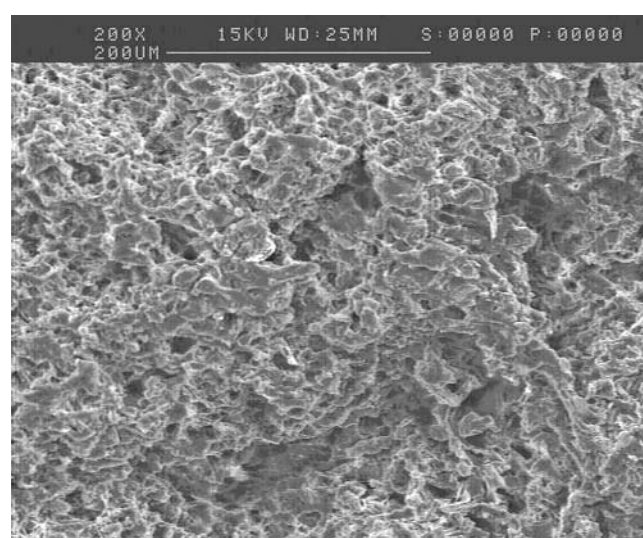


(b)

**Figure 6.** Scanning electron micrographs of tensile fracture surface of PP/EPDM/PS composite with: (a) 30 wt% and (b) 60 wt % of PS (magnification 200X).



(a)



(b)

**Figure 7.** Scanning electron micrographs of tensile fracture surface of PP/EPDM/kaolin composite with: (a) 30 wt % and (b) 60 wt % of kaolin (magnification 200X).

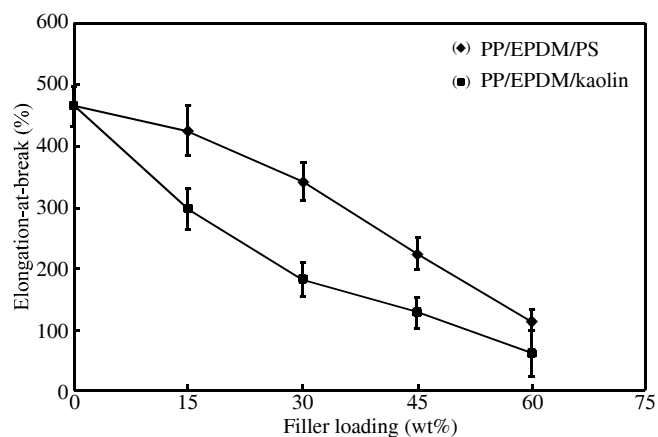
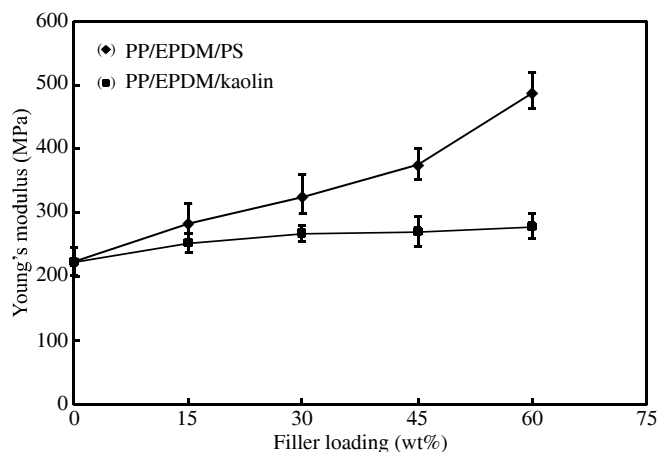


**Figure 8.** Effect of filler loading on elongation-at-break of PP/EPDM/PS and PP/EPDM/kaolin composites.

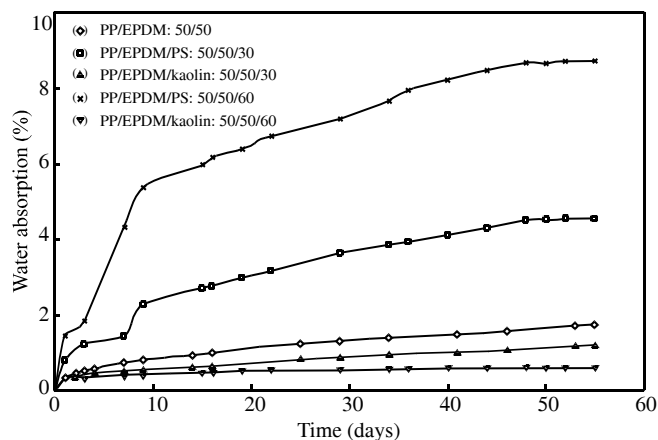
(Figure 8) than PP/EPDM/PS composites.

Figure 9 shows the effect of filler loading on Young's modulus of PP/EPDM/PS and PP/EPDM/kaolin composites. The Young's modulus of both composites increases with increasing filler loading, Young's modulus is an indication of relative stiffness of composites [22]. At a similar filler loading Young's modulus of PP/EPDM/PS composites show significantly higher value than PP/EPDM/kaolin composites. It can be seen that the addition of paper sludge gives beneficial effect significantly by improving the stiffness of PP/EPDM/PS composites compared to PP/EPDM/kaolin composites.

Figure 10 shows the typical water absorption curves versus time at different filler loading of PP/EPDM/PS and PP/EPDM/kaolin composites. All composites show a similar pattern of water absorption



**Figure 9.** Effect of filler loading on Young's modulus of PP/EPDM/PS and PP/EPDM/kaolin composites.



**Figure 10.** Percentage of water absorption vs. time of PP/EPDM composites with different filler loading.

(except PP/EPDM); that is, initial sharp water up take followed by gradual increment, until equilibrium water content was achieved at about 50 days. However, composites with higher paper sludge loading show more water absorption. As shown in Table 2, paper sludge consists of 59% of organic components (cellulose, hemicellulose and lignin) and 10% of silica. As filler

**Table 2.** Semi quantitative analysis of paper sludge using X-ray fluorescence spectrometer Rigaku RIX 3000.

Component	wt (%)
Na <sub>2</sub> O	0.057
MgO	3.0
Al <sub>2</sub> O <sub>3</sub>	7.1
SiO <sub>2</sub>	10.0
P <sub>2</sub> O <sub>5</sub>	0.065
SO <sub>3</sub>	0.14
Cl <sub>2</sub> O	0.19
K <sub>2</sub> O	0.035
CaO	20.0
TiO <sub>2</sub>	0.11
MnO	0.018
Fe <sub>2</sub> O <sub>3</sub>	0.19
ZnO	0.017
SrO	0.011
LOI (Organic)	59.0

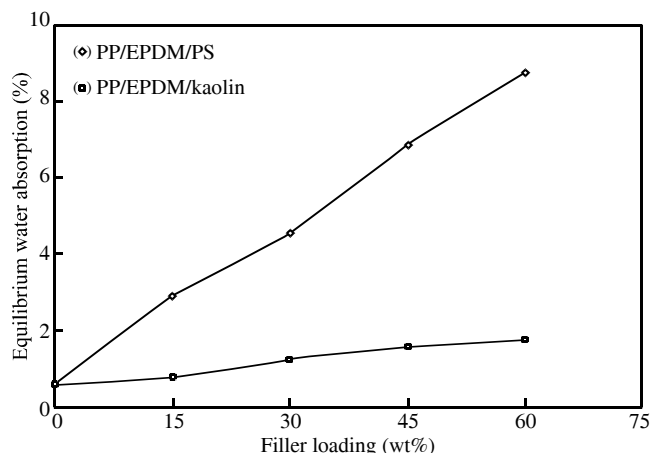


**Figure 11.** Percentage of equilibrium swelling vs. filler loading of PP/EPDM/PS and PP/EPDM/kaolin composites.

content increases, the number of hydrogen bonds between organic components and silica with water molecules increases.

Figure 11 shows the variation of equilibrium swelling at 55 days immersion in water with filler loading for PP/EPDM/PS and PP/EPDM/kaolin composites. It can be seen that at a similar filler loading, PP/EPDM/PS composites exhibit higher water absorp-

**Table 3.** Semi quantitative analysis of kaolin using X-ray fluorescence spectrometer Rigaku RIX 3000.

Component	wt (%)
MgO	0.33
Al <sub>2</sub> O <sub>3</sub>	30
SiO <sub>2</sub>	63
P <sub>2</sub> O <sub>5</sub>	0.065
SO <sub>3</sub>	0.030
K <sub>2</sub> O	1.5
CaO	0.042
TiO <sub>2</sub>	0.025
Fe <sub>2</sub> O	0.84
NiO	0.012
Br <sub>2</sub> O	0.59
Rb <sub>2</sub> O	0.044
ZrO <sub>2</sub>	0.018
LOI	3.5

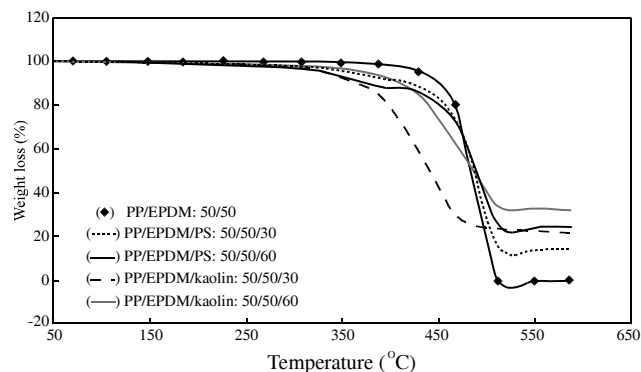


**Figure 12.** Thermogravimetric analysis curves of PP/EPDM/PS composites with different filler loading.

tion than PP/EPDM/kaolin composites. Cellulose fibres (organic material) are hydrophilic in nature, and therefore they can absorb water, which leads to a weight increases. The tendency of organic materials to form hydrogen bonds with water molecules is higher than inorganic materials. As is shown in Tables 2 and 3, paper sludge has higher organic components than kaolin.

Figure 12 shows the typical thermal degradation of PP/EPDM, PP/EPDM/PS, and PP/EPDM/kaolin composites at 0, 30, and 60 wt% of filler loading. It can be seen that the initial decomposition temperature of both composites reduces with increasing filler loading. Table 4 shows that the percentage weight loss of PP/EPDM, PP/EPDM/PS, and PP/EPDM/kaolin composites at different temperature and filler loading. The total weight loss of PP/EPDM/kaolin composites is lower than PP/EPDM/PS composites, which might be due to the presence of large content of inorganic materials in kaolin (about 96%) compared to paper sludge,

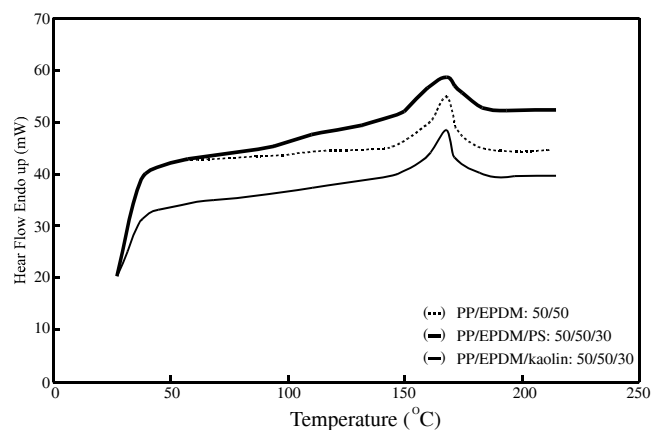


**Figure 13.** Differential scanning calorimetric curve of PP/EPDM/PS composites with different filler loading.

**Table 4.** Percentage weight loss of PP/EPDM, PP/EPDM/PS, and PP/EPDM/kaolin composites at different temperatures.

Temperature (°C)	Weight loss (%)				
	PP/EPDM (50/50)	PP/EPDM/PS (50/50/30)	PP/EPDM/PS (50/50/60)	PP/EPDM/kaolin (50/50/30)	PP/EPDM/kaolin (50/50/60)
100	0.05	0.18	0.25	0.089	0.604
150	0.031	0.41	0.47	0.128	0.212
200	0.052	0.47	0.81	0.113	0.289
250	0.093	0.22	0.3	0.907	0.236
300	0.188	0.73	1.07	1.678	0.651
350	0.450	2.43	3.7	4.492	1.655
400	1.283	3.82	5.36	14.92	4.091
450	7.341	8.22	7.09	35.55	16.20
500	82.94	60.08	49.78	18.83	40.89
550	7.57	6.01	6.37	1.71	2.20
Total weight loss (%)	100	82.6	75.2	78.4	67

**Table 5.** The thermal parameter DSC of PP/EPDM, PP/EPDM/PS, and PP/EPDM/kaolin composites.

Sample	Melting temperature	$\Delta H_{f(\text{com})}$	$X_{\text{com}}$	$X_{\text{pp}}$
	$T_m$ (°C)	(J/g)	(% crystallinity)	(%)
PP/EPDM (50/50)	167.1	40.07	19.2	38.4
PP/EPDM/PS (50/50/30)	167.3	36.45	17.4	45.1
PP/EPDM/PS (50/50/60)	167.5	35.35	16.9	54.1
PP/EPDM/kaolin (50/50/30)	167.3	27.89	13.3	34.5
PP/EPDM/kaolin (50/50/60)	167.2	27.52	13.1	41.9

which consists of about 41% inorganic materials.

Figure 13 shows the typical DSC curve of PP/EPDM, PP/EPDM/PS, and PP/EPDM/kaolin composites at 0 and 30 wt% of filler loading. Whereas Table 5 indicates the value of melting temperature ( $T_m$ ), heat fusion of composites ( $\Delta H_{f(\text{com})}$ ), crystallinity of composites ( $X_{\text{com}}$ ), and crystallinity of PP ( $X_{\text{pp}}$ ) for PP/EPDM, PP/EPDM/PS, and PP/EPDM/kaolin composites. The results show that the percentage of crystallinity of both composites changed with filler loading. It can be seen that the value of  $\Delta H_{f(\text{com})}$  and  $X_{\text{com}}$  decrease with increasing filler loading. This is due to the decreasing of PP content at higher filler loadings. The addition of both fillers increase  $X_{\text{pp}}$  value. This observation was due to the nucleating ability of both fillers in the crystallization of PP. However from

Table 5, at a similar filler loading, PP/EPDM/PS composites exhibit higher  $X_{\text{com}}$  and  $X_{\text{pp}}$  values than PP/EPDM/kaolin composites. This might be due to the better nucleation effect of paper sludge over kaolin. The similar observation was reported by Xiuying et al. [17]. It can be seen also from Table 5, that the incorporation of both fillers does not affect the melting temperature of the composites.

## CONCLUSION

The mechanical properties, water absorption, morphology, and thermal properties of PP/EPDM/paper sludge composites were investigated and compared with PP/EPDM/kaolin composites. It was found that



PP/EPDM/kaolin composites exhibit higher tensile strength, elongation-at-break, lower water absorption, and better initial degradation temperature than PP/EPDM/PS composites. The SEM tensile fracture surfaces of PP/EPDM/kaolin show better filler-matrix interfacial interaction than PP/EPDM/PS composites. However, PP/EPDM/PS composites show higher Young's modulus and percentage of crystallinity than PP/EPDM/kaolin composites. This indicates that the paper sludge has a better nucleation effect than kaolin.

## REFERENCES

1. Chi Ming C., Jing S.W., Jian X, L., Ying K.C., Polypropylene/calcium carbonate nanocomposites, *Polymer*, **43**, 2981- 2992 (2002).
2. Da Silva A.L.N., Rocha M.C.G., Moraes M.A.R., Valente C.A.R., Mechanical and rheological properties of composites based on polyolefin and mineral additives *Polym. Test.*, **21**, 57-60 (2001).
3. Petrovic Z.S., Javni I., Waddon A., Banhegi G., Structure and properties of polyurethane-silica nanocomposite, *J. Appl. Polym. Sci.*, **76**, 133-151 (2000).
4. Rong M.Z., Zhang M.Q., Zheng Y.X., Zeng H.M, Walter R., Friedrich K., Structure property relationship of irradiation grafted nano-inorganic particle filled polypropylene composite, *Polymer*, **42**, 167-183 (2001).
5. Ismail H., Rozman H.D., Studies on the tensile properties of rubberwood fibre-natural rubber, *Int. J. Polym. Mater.*, **41**, 325-333 (1998).
6. Ismail H., Salmah, Nasir M., Dynamic vulcanization of rubberwood-filled polypropylene/natural rubber blends, *Polym. Test.*, **20**, 819-823 (2001).
7. Ismail H., Salmah, Nasir M., The effect of dynamic vulcanization on mechanical properties and water absorption of silica and rubberwood filled polypropylene/natural rubber hybrid composites, *Int. J. Polym. Mater.*, **53**, 229-238 (2003).
8. Ismail H., The potential of rubberwood as a filler in epoxidized natural rubber compounds, *J. Elasto. Plast.*, **33**, 34-46 (2001).
9. Ismail H., Rozman H.D., Jaffri R.M., Mohd Ishak Z.A., Oil palm wood flour reinforced epoxidized natural rubber composite: The effect of filler content and size, *Eur. Polym. J.*, **33**, 1627-1632 (1997).
10. Gasan J., Bledzki A. K., The influence of fiber-surface treatment on the mechanical properties of jute-polypropylene composites, *Composite: Part A*, **28A**, 1001-1005 (1997).
11. Ismail H., Shuhelmy S., Edyham M. R., The effect of a silane coupling agent on curing characteristics and mechanical properties of bamboo fibre filled NR composites, *Eur. Polym. J.*, **38**, 39-47 (2002).
12. Ismail H., The effect of filler loading and silane coupling agent on dynamic properties and swelling behaviour of bamboo filled NR compounds, *J. Elasto. Plast.*, **35**, 149 (2003).
13. Chuai C. Z., Almdal K., Poulsen L., Plackett D., Conifer fibers as reinforcing material for polypropylene-based composites, *J. Appl. Polym. Sci.*, **80**, 2833-2841 (2001).
14. Jungil S., Hyun-Joong K., Phil-Woo L., Role of paper sludge particle size and extrusion temperature on performance of paper sludge-thermoplastic polymer composites, *J. Appl. Polym. Sci.*, **82**, 2709-2718 (2001).
15. Jang J., Lee E., Improvement of the flame retardancy of paper-sludge/polypropylene composites, *Polym. Test.*, **20**, 7-13 (2001).
16. Xiuying Q., Yong Z., Yinxi Z., Yutang Z., Ink-eliminated waste paper sludge flour-filled polypropylene composites with different coupling agent treatments, *J. App. Polym. Sci.*, **89**, 513-520 (2003).
17. Xiuying Q., Yong Z., Yinxi Z., Ink-eliminated paper sludge flour as filler for polypropylene, *Polym. Polym. Compos.*, **11**, 321-326 (2003).
18. Greco R., Manacarella C., Martuscelli E., Ragosta G., Polyolefin blends: 2. Effect of EPR composition on structure, morphology and mechanical properties of iPP/EPR alloys, *Polymer*, **28**, 1929- 1936 (1987).
19. Shonaik G.O., Kiat T.H., Studies on miscibility of uncompatibilized nylon 66-santoprene blends, *J. App. Polym. Sci.*, **68**, 350-357 (1998).
20. Ismail H., Salmah, Bakar A.A., The effect of paper sludge on processibility, swelling behaviour and morphology of polypropylene (PP)/ ethylene propylene diene terpolymer (EPDM) composites, *J. Reinf. Plast. Comp.*, **2**, 147-159 (2005).
21. Katz H.S., Milewski J.V., *Handbook of Fillers and Reinforcements for Plastics*, Van Nostrand Reinhold, London, 136 (1987).
22. Shah V., *Handbook of Polymer Testing*, Wiley Interscience, New York, 7 (1983).